Electronic Supplementary Material (ESI) for Inorganic Chemistry Frontiers.

Modulation of the magnetic anisotropy of octahedral cobalt(II) single-ion magnets by a fine-tuning of axial coordination microenvironment

Yuewei Wu,[a#] Danian Tian,[d#] Jesús Ferrando-Soria,[b] Joan Cano,[b] Lei Yin,[c] Zhongwen Ouyang,[c] Zhenxing Wang,*[c] Shuchang Luo,[e] Xiangyu Liu,*[a,b] and Emilio Pardo[b]

[a] State Key Laboratory of High-efficiency Utilization of Coal and Green Chemical Engineering, College of Chemistry and Chemical Engineering, Ningxia University, Yinchuan 750021, China

[b] Departamento de Química Inorgánica, Instituto de Ciencia Molecular (ICMOL), Universidad de Valencia, Paterna 46980, Valencia, Spain.

[c] Wuhan National High Magnetic Field Center & School of Physics, Huazhong University of Science and Technology, Wuhan, 430074, China

[d] College of Public Health and Management, Ningxia Medical University, Yinchuan 750021, China

[e] College of Chemical Engineering, Guizhou University of Engineering Science, Bijie 551700, China

# These authors contributed equally to this work.

***Corresponding author**
Dr. Xiangyu Liu
E-mail: xiangyuliu432@126.com

Prof. Zhenxing Wang
E-mail: zxwang@hust.edu.cn

Table of contents

Table S1. Selected Bond Lengths (Å) and Bond Angles (°) for **1**

		1			
Co(1)-O(2W)	2.096(3)	Co(2)-O(1)	2.117(3)	O(2W) -Co(1)-O(3)#1	89.75(9)
Co(1)-O(3)	2.119(3)	Co(2)-O(1W)	2.095(3)	O(3)-Co(1)-N(1)	88.70(12)
Co(1)-O(2W)#1	2.096(3)	Co(2)-N(3)#2	2.174(3)	N(1)-Co(1)-N(1)#1	180.00(11)
Co(1)-O(3)#1	2.119(3)	Co(2)-N(3)	2.174(3)	O(1) -Co(2)-N(3)	92.09(13)
Co(1)-N(1)	2.158(3)	Co(1)-Co(1)	14.130	O(1)#2-Co(2)-N(3)	87.91(13)
Co(1)-N(1)#1	2.158(3)	N(1)-C(5)	1.333(4)	O(1W)-Co(2)-O(1)	91.50(9)
Co(2)-O(1W)#2	2.095(3)	N(1)-C(1)	1.342(4)	C(5)-N(1)-C(1)	116.0(3)
Co(2)-O(1)#2	2.117(3)	C(1)-C(2)	1.366(5)	N(1)-C(1)-C(2)	123.1(3)
#1 -x,-y+1,-z+1	#2 -x+1,-y,-z				

Table S2. Selected Bond Lengths (Å) and Bond Angles (°) for **2**

	2		
Co(1)-O(1)	2.065(13)	O(1) -Co(1)-O(1W)#1	180.0
Co(1)-O(1)#1	2.065(13)	O(1)-Co(1)-N(1)#1	90.39(6)
Co(1)-O(1W)	2.122(13)	N(1)#1-Co(1)-N(1)	180.0
Co(1)-O(1W)#1	2.122(13)	O(1W)-Co(1)-N(1)	87.12(6)
Co(1)-N(1)	2.2022(17)	O(1)#1-Co(1)-N(1)	90.39(6)
Co(1)-N(1)#1	2.2022(17)	O(1)-Co(1)-N(1)	89.61(6)
#1 –x+2,-y,-z+2			

Table S3. Hydrogen-bonded parameters /Å, ° for complexes **1** and **2**

Complex	D–H···A	D–H	H···A	D···A	DHA
1	O1W–H1WB···N4	0.920	1.838	2.752	172
	O2W–H2WB···N2	0.915	1.841	2.749	171
2	O1W–H1WB···N2	0.759	2.030	2.783	172

Table S4. Co(II) ion geometry analysis of **1** and **2** by SHAPE 2.1 software

Configuration	ABOXIY, **1**(Co1)	ABOXIY, **1**(Co2)	ABOXIY, **2**
OC-6	0.025	0.076	0.117
TPR-6	16.520	16.155	16.427
JPPY-6	33.423	33.195	32.529

Table S5 Relaxation fitting parameters from least-squares fitting of $\chi(f)$ data under 2000 Oe dc field of **1**

T(K)	χ_T	χ_S	α
3	0.213	0.006	0.15
3.5	0.186	0.006	0.105
4	0.163	0.006	0.069
4.5	0.146	0.005	0.037
5	0.132	0.003	0.026
5.2	0.127	0.003	0.049
5.5	0.120	0.002	0.031
5.8	0.114	0.006	0.018
6	0.111	0.001	0.02

Table S6 Relaxation fitting parameters from least-squares fitting of $\chi(f)$ data under 2000 Oe dc field of **2**

T(K)	χ_T	χ_S	α
2	0.367	0.006	0.17
2.5	0.331	0.007	0.15
3	0.295	0.004	0.138
3.5	0.259	0.003	0.08
4	0.231	0.003	0.05
4.2	0.221	0.007	0.05
4.5	0.209	0.003	0.10
5	0.188	0.003	0.03

Table S7 Energy levels (cm^{-1}) of ligand field multiplets in zero field derived from CASSCF/NEVPT2/def2-TZVP(f) CASSCF(7,5) (ORCA) calculations for the complex **1**

0	0.0	30	15909.3	60	26899.5	90	36511.5
1	0.0	31	15909.3	61	26899.5	91	36511.5
2	182.0	32	20211.2	62	27294.5	92	36844.0
3	182.0	33	20211.2	63	27294.5	93	36844.0
4	648.9	34	20529.5	64	29429.0	94	37296.4
5	648.9	35	20529.5	65	29429.0	95	37296.4
6	948.1	36	20860.7	66	29804.0	96	47678.4
7	948.1	37	20860.7	67	29804.0	97	47678.4
8	1428.2	38	21166.0	68	29990.5	98	48102.0
9	1428.2	39	21166.0	69	29990.5	99	48102.0
10	1535.1	40	21517.1	70	30256.6	100	48384.2
11	1535.1	41	21517.1	71	30256.6	101	48384.2
12	6965.0	42	21610.1	72	30397.3	102	48992.8
13	6965.0	43	21610.1	73	30397.3	103	48992.8
14	7012.5	44	23788.7	74	30655.8	104	49102.9
15	7012.5	45	23788.7	75	30655.8	105	49102.9
16	7340.2	46	23833.1	76	32384.3	106	49546.6
17	7340.2	47	23833.1	77	32384.3	107	49546.6
18	7407.4	48	24220.3	78	32801.4	108	50029.1
19	7407.4	49	24220.3	79	32801.4	109	50029.1
20	7756.9	50	24351.4	80	35034.9	110	73291.5
21	7756.9	51	24351.4	81	35034.9	111	73291.5
22	7857.0	52	24945.2	82	35346.8	112	73559.7
23	7857.0	53	24945.2	83	35346.8	113	73559.7
24	14963.8	54	25196.0	84	35647.8	114	74017.4
25	14963.8	55	25196.0	85	35647.8	115	74017.4
26	15104.7	56	25464.5	86	36202.2	116	74411.2
27	15104.7	57	25464.5	87	36202.2	117	74411.2
28	15106.9	58	26718.2	88	36394.6	118	74679.1
29	15106.9	59	26718.2	89	36394.6	119	74679.1

Table S8 Individual contributions to *D*-tensor for **1** by CASSCF/NEVPT2/def2-TZVP(-f) CASSCF(7,5) (ORCA).

2*S*+1	Root	*D*	*E*	2*S*+1	Root	*D*	*E*
4	0	0.000	0.000	2	15	-0.433	0.308
4	1	48.511	48.196	2	16	-0.244	-0.243
4	2	27.994	-27.447	2	17	-0.339	-0.266
4	3	-7.150	-1.522	2	18	0.088	0.409
4	4	1.000	-0.724	2	19	-0.307	-0.282
4	5	-3.955	2.259	2	20	0.451	0.045
4	6	0.001	-0.001	2	21	-0.078	-0.116
4	7	0.028	0.028	2	22	-0.123	0.095
4	8	0.059	-0.054	2	23	0.036	-0.029
4	9	0.029	0.025	2	24	0.045	-0.002
2	0	-1.153	0.503	2	25	0.033	-0.050
2	1	-0.556	-0.375	2	26	0.044	0.004
2	2	-0.117	-0.114	2	27	-0.068	0.039
2	3	-0.075	0.057	2	28	-0.017	0.058
2	4	-1.054	-1.048	2	29	0.035	-0.027
2	5	-0.617	0.513	2	30	0.118	-0.010
2	6	-0.216	0.216	2	31	-0.051	-0.050
2	7	-0.401	0.363	2	32	-0.033	0.037
2	8	3.104	0.003	2	33	-0.037	-0.002
2	9	-0.090	0.024	2	34	-0.001	0.000
2	10	-0.051	-0.007	2	35	-0.018	-0.018
2	11	-0.033	0.028	2	36	0.001	0.001
2	12	0.352	0.040	2	37	0.001	0.000
2	13	0.176	0.022	2	38	-0.002	-0.002
2	14	-0.032	0.047	2	39	-0.016	0.023

Table S9 Energy levels (cm^{-1}) of ligand field multiplets in zero field derived from CASSCF/NEVPT2/def2-TZVP(f) CASSCF(7,5) (ORCA) calculations for the complex **2**

0	0.0	30	18286.9	60	24398.5	90	36847.3
1	0.0	31	18286.9	61	24398.5	91	36847.3
2	269.4	32	18891.2	62	26131.9	92	37169.9
3	269.4	33	18891.2	63	26131.9	93	37169.9
4	518.4	34	19091.2	64	28672.0	94	37482.1
5	518.4	35	19091.2	65	28672.0	95	37482.1
6	895.0	36	19344.5	66	29028.7	96	42762.9
7	895.0	37	19344.5	67	29028.7	97	42762.9
8	1292.6	38	19911.4	68	29189.9	98	43366.8
9	1292.6	39	19911.4	69	29189.9	99	43366.8
10	1377.9	40	20278.3	70	30011.4	100	44123.5
11	1377.9	41	20278.3	71	30011.4	101	44123.5
12	8390.3	42	20711.9	72	30225.6	102	44854.9
13	8390.3	43	20711.9	73	30225.6	103	44854.9
14	8441.4	44	21207.7	74	30445.7	104	45408.3
15	8441.4	45	21207.7	75	30445.7	105	45408.3
16	8967.0	46	21320.0	76	31994.3	106	45861.9
17	8967.0	47	21320.0	77	31994.3	107	45861.9
18	9009.2	48	22265.6	78	32446.5	108	46037.1
19	9009.2	49	22265.6	79	32446.5	109	46037.1
20	9323.9	50	22510.9	80	34686.5	110	65692.9
21	9323.9	51	22510.9	81	34686.5	111	65692.9
22	9432.7	52	23046.9	82	35094.1	112	66506.1
23	9432.7	53	23046.9	83	35094.1	113	66506.1
24	11183.5	54	23528.7	84	35516.0	114	67056.2
25	11183.5	55	23528.7	85	35516.0	115	67056.2
26	12985.6	56	23700.7	86	36179.4	116	67480.9
27	12985.6	57	23700.7	87	36179.4	117	67480.9
28	18270.6	58	24138.4	88	36632.8	118	67852.6
29	18270.6	59	24138.4	89	36632.8	119	67852.6

Table S10 Individual contributions to *D*-tonsor for **2** by CASSCF/NEVPT2/def2-TZVP(-f) CASSCF(7,5) (ORCA)

2*S*+1	Root	*D*	*E*	2*S*+1	Root	*D*	*E*
4	0	0.000	0.000	2	15	-0.039	0.039
4	1	66.971	66.581	2	16	-0.500	0.463
4	2	33.001	-32.417	2	17	-0.635	-0.607
4	3	1.724	0.287	2	18	1.566	0.204
4	4	2.970	2.634	2	19	0.440	-0.021
4	5	2.122	-1.685	2	20	0.177	0.234
4	6	0.000	-0.001	2	21	-0.265	-0.129
4	7	0.048	-0.041	2	22	-0.221	0.004
4	8	0.034	0.015	2	23	-0.135	0.122
4	9	0.012	0.012	2	24	-0.006	-0.009
2	0	7.513	1.273	2	25	0.295	-0.040
2	1	0.568	-0.189	2	26	-0.083	-0.021
2	2	-0.025	-0.015	2	27	-0.013	-0.031
2	3	-0.081	0.073	2	28	-0.004	0.004
2	4	-1.001	-0.915	2	29	-0.039	-0.043
2	5	-0.439	-0.082	2	30	0.021	0.001
2	6	-0.868	0.858	2	31	-0.105	0.051
2	7	-0.099	0.094	2	32	-0.107	-0.058
2	8	2.875	0.000	2	33	-0.001	0.000
2	9	-0.160	-0.140	2	34	0.002	0.000
2	10	-0.019	-0.019	2	35	0.014	-0.003
2	11	-0.079	0.091	2	36	0.000	0.000
2	12	0.130	0.015	2	37	0.002	0.000
2	13	0.059	0.049	2	38	-0.005	0.007
2	14	-0.013	0.013	2	39	0.133	0.017

Table S11. ZFS parameters and relaxation parameters with easy-plane anisotropy of octahedral Co(II) ion.

Complexes	Chromophore	Axial bond distances	equatorial bond lengths	D/cm^{-1}		DC field/Oe	U_{eff}/K	τ_0/s	Ref.
				$D^{[a]}$	$D^{[b]}$				
[Co(2-Himap)$_2$] (**3**)	CoN_4O_2	2.115	2.091	+36.7	+39.3	2000	14	5×10^{-4}	44
[Co(3,5-dnb)$_2$(py)$_2$(H$_2$O)$_2$](the *C2/c* Polymorph) (**4**)	CoN_2O_4	2.141	2.104	+58	+91.5	1000	28.0	1.37×10^{-7}	21
[Co(3,5-dnb)$_2$(py)$_2$(H$_2$O)$_2$](the *P2$_1$/c* Polymorph) (**5**)	CoN_2O_4	2.151	2.109	+68	+117.4	1000	30.3	3.4×10^{-8}	21
{[Co(bimb)(H$_2$O)$_4$]·(L2)·2DMF}$_n$ (**6**)	CoN_2O_4	2.183	2.093	+57.5	-	2000	8.82	2.60×10^{-6}	17
{[Co(3,3′-Hbpt)$_2$(SCN)$_2$]·2H$_2$O}$_n$ (**7**)	$CoN_4N'_2$	2.068	2.210	+70.1	+82	1500	105	3.22×10^{-8}	45
[Co(abpt)$_2$(tcm)] (**8**)	$CoN_4N'_2$	2.133	2.117	+48	+53.7	3000	86.2	1.37×10^{-9}	46
[Co(H$_2$pimdc)$_2$(phen)]$_n$ (**9**)	CoN_4O_2	2.119	2.126	+3.47	+82.82	2000	48.49	3.79×10^{-8}	47
[Co(9Accm)$_2$(py)$_2$] (**10**)	CoN_2O_4	2.209	2.018	+74.1	+167.1(146.5)	1500	-	-	48
[Co(9Accm)$_2$(2,2'-bpy)] (**11**)	CoN_2O_4	2.092	2.064	+24.1	+71.6(50.2)	700	-	-	48
{[Co(bmzbc)$_2$]·2DMF}$_n$ (**12**)	CoN_2O_4	2.109	2.15	+60.6	+62.6	1000	11.8	1.3×10^{-5}	49
[Co(L^1)$_2$](ClO$_4$)$_2$ (**13**)	CoN_6	2.153	2.117	+61.1	+68.9	2000	14.8	7.18×10^{-7}	25
[Co(L^2)$_2$](ClO$_4$)$_2$ (**14**)	CoN_6	2.180	2.116	+68.1	+67.3	2000	27.3	2.06×10^{-8}	25
[Co(L^2)$_2$](ClO$_4$)$_2$·MeCN (**15**)	CoN_6	2.183	2.139	+56.4	+71.5	2000	22.6	3.44×10^{-7}	25
[Co(L^4)$_2$](ClO$_4$)$_2$ (**16**)	CoN_6	2.195	2.134	+62.9	+85.0	2000	20.4	4.95×10^{-7}	25
[Co(L^5)$_2$](ClO$_4$)$_2$ (**17**)	CoN_6	2.180	2.120	+74.9	+72.1	2000	8.0	1.67×10^{-6}	25
NEt$_4$[Co(hfac)$_3$] (**18**)	CoN_6	2.050	2.079	+117.8	+121.2	1000	20.6	6.5×10^{-7}	50
[Co(pydm)$_2$](dnbz)$_2$ (**19**)	CoN_2O_4	2.038	2.142	+44	-95	2000	39	8×10^{-9}	51
[Co(dppm^{O,O})$_3$][CoBr$_4$] (**20**)	CoO_6	2.091	2.106	+147	+129	4000	-	-	52
[Co(2,6-dfba)$_2$(TMD)$_2$(H$_2$O)$_2$]$_n$ (**1**)	CoN_2O_4	2.166	2.107	+53.19	+85.16	2000	45.34	1.67×10^{-8}	This work
[Co(2,6-dfba)$_2$(VND)$_2$(H$_2$O)$_2$]$_n$ (**2**)	CoN_2O_4	2.2022	2.094	+65.67	+122.23	2000	57.97	1.88×10^{-8}	This work

[a] Axial magnetic anisotropy obtained from the fit of the experimental field dependence of magnetization data; [b] Axial magnetic anisotropy obtained from theory calculations. Abbreviations: 2-Himap = *o*-[(1*H*-imidazol-2-yl)methylideneamino]phenol; 3,5-dnb = 3,5-dinitrobenzoic acid; py = pyridine; bimb = 1,4-bis(benzoimidazo-1-ly)benzene; H$_2$L2 = 2,2’-(1,4-phenylenebis(methylene))bis(sulfanediyl)dinicotinic acid; 3,3′-Hbpt = 1H-3-(3-pyridyl)-5-(3′-pyridyl)-1,2,4-triazole; abpt = 4-amino-3,5-bis(2-pyridyl)-1,2,4-triazole; tcm = tricyanomethanide Anion; H$_2$pimdc = 2-propyl-imidazole-4,5-dicarboxylate; phen = 1,10-phenanthroline monohydrate; 9Accm = 1,7-Bis(9-anthryl)-1,6-heptadiene-3,5-dionate; 2,2′-bpy = 2,2′-bipyridyl; bmzbc = 4-(benzimidazole-1-yl)benzoate; L^1 = pyridine-2,6-bis(oxazoline); L^2 = pyridine-2,6-bis(5,5’-dimethyloxazoline); L^4 = 4-(4-methyl)-phenyl-pyridine-2,6-bis(5,5’-dimethyloxazoline); L^5 = 4,4’-bipyridine-2,6-bis(5,5’-dimethyloxazoline); hfac = hexafluoroacetylacetonate; pydm = 2,6-pyridinedimethanol; dnbz = 3,5-dinitrobenzoato; dppm^{O,O} = bis(diphenylphosphanoxido)methane.

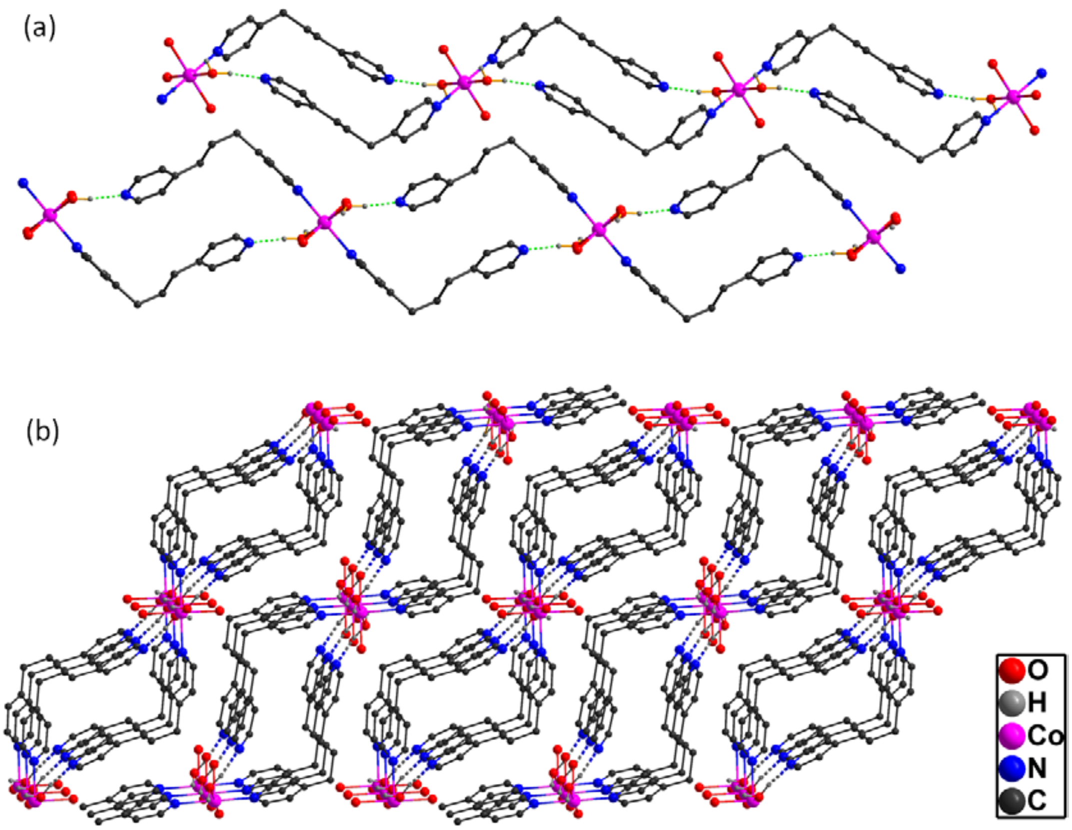

Fig. S1 1D chains formed via intermolecular hydrogen bonds (a) and the 3D supramolecular networks (b) of complex **1**. H atoms and 2,6-dfba$^-$ ions are omitted for clarity.

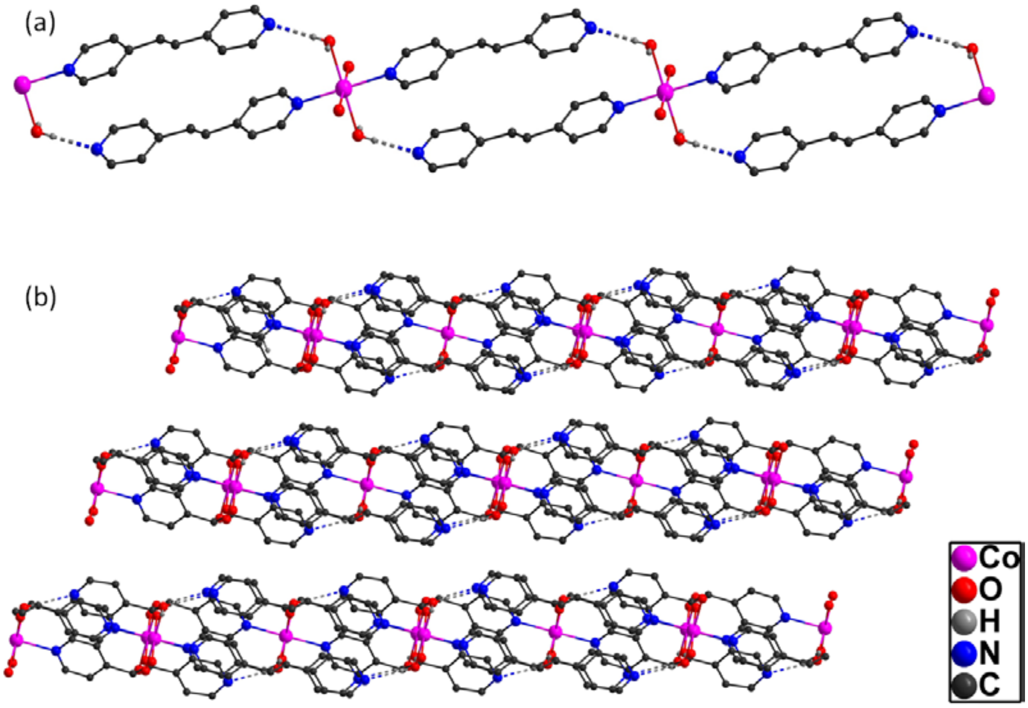

Fig. S2 1D chain formed via intermolecular hydrogen bonds (a) and the 3D supramolecular networks (b) of complex **2**. H atoms and 2,6-dfba$^-$ ions are omitted for clarity.

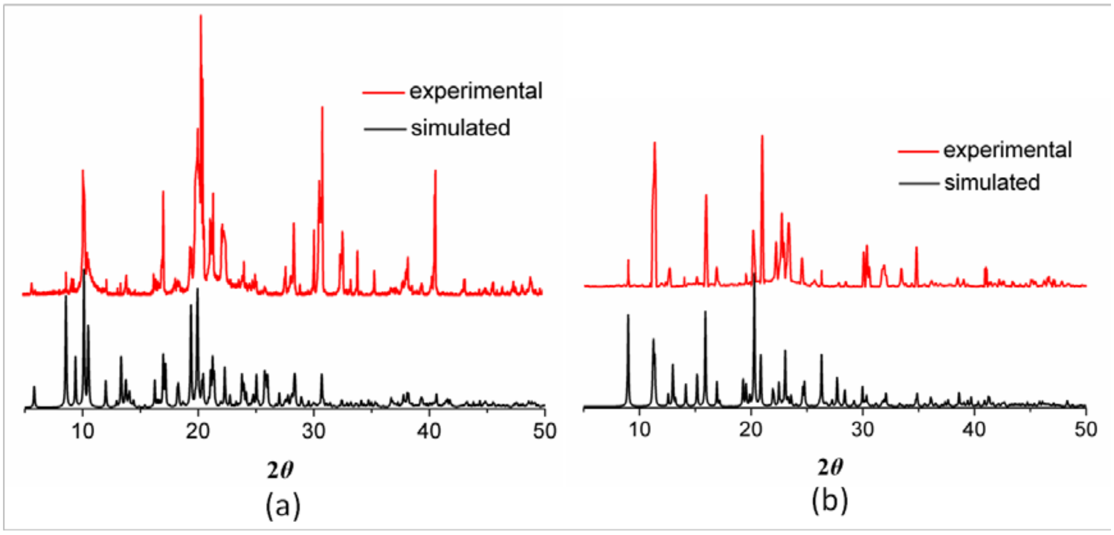

Fig. S3 PXRD patterns for complexes **1** (a) and **2** (b).

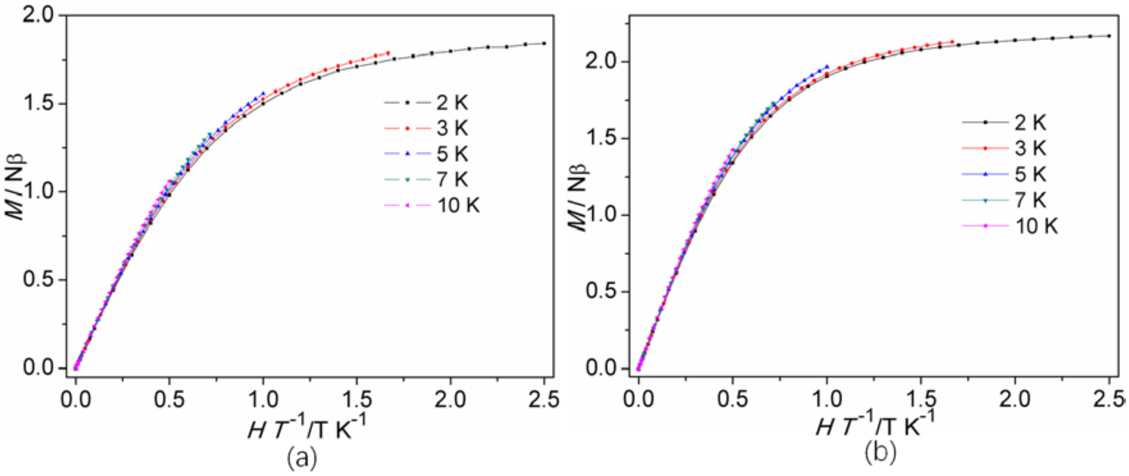

Fig. S4 Plots of *M* vs *H*/*T* for **1** (a) and **2** (b) at different temperatures.

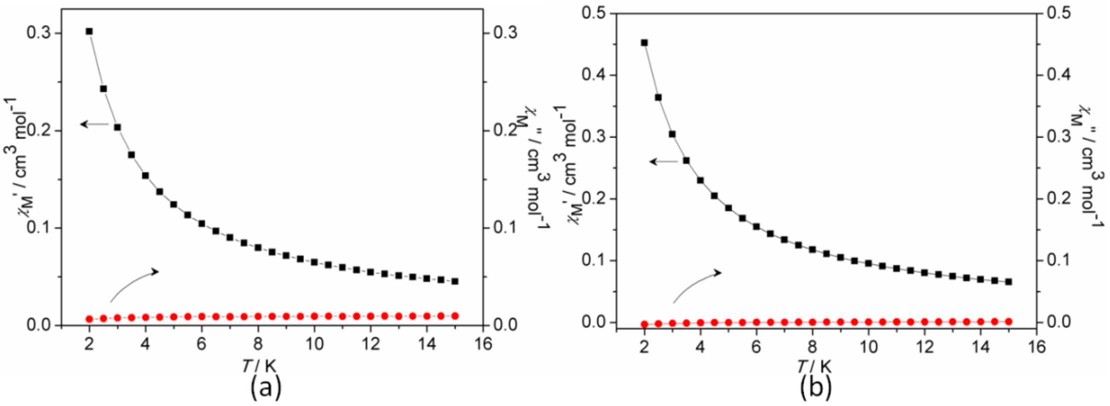

Fig. S5 Ac magnetic susceptibility measurements for **1** (a) and **2** (b) in 0 Oe static field.

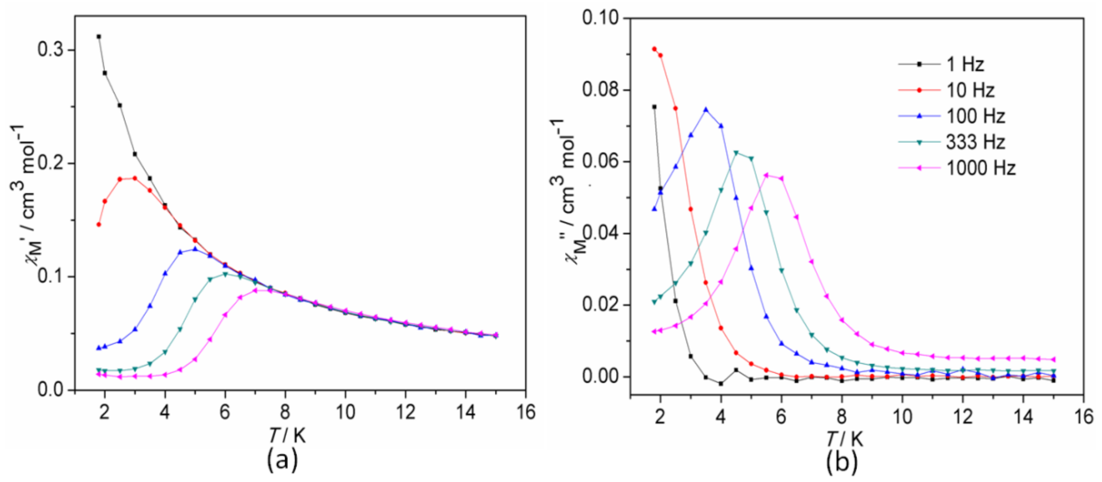

Fig. S6 Temperature dependence of the in-phase (a) and out-of-phase (b) ac susceptibilities at different frequencies with a dc field of 2000 Oe for complex **1**.

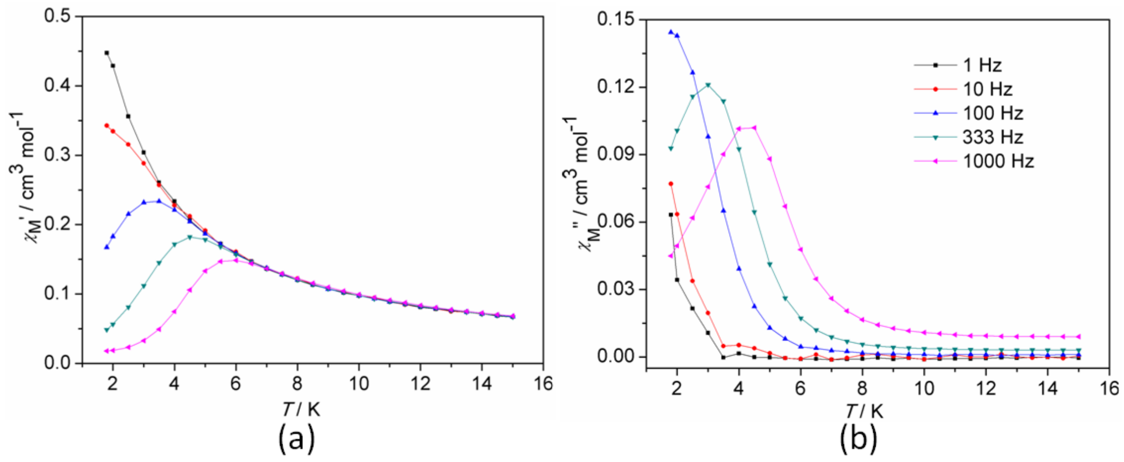

Fig. S7 Temperature dependence of the in-phase (a) and out-of-phase (b) ac susceptibilities at different frequencies with a dc field of 2000 Oe for complex **2**.

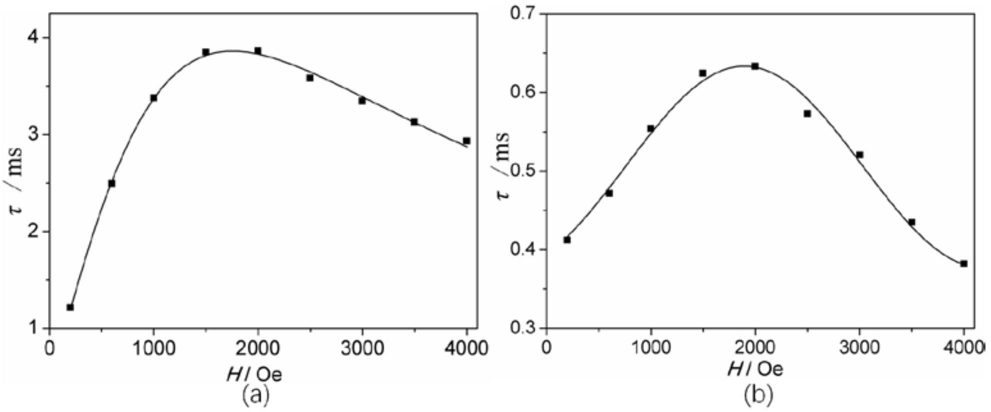

Fig. S8 Field dependence of the magnetic relaxation time at 3 K for **1** (a) and **2** (b).